EPSC Abstracts
Vol. 11, EPSC2017-28-1, 2017
European Planetary Science Congress 2017

An exceptionally high standing ridge on Enceladus

B. Giese (1), P. Helfenstein (2), E. Hauber (1), H. Hussmann (1) and R. Wagner (1)
(1) Institute of Planetary Research, DLR, Berlin, Germany
(2) Cornell Center for Astrophysics and Planetary Science, Ithaca, USA (bernd.giese@dlr.de)

Abstract

Cassini stereo-derived topography reveals an exceptionally high-standing saw-tooth-shaped ridge in Enceladus' Samarkand Sulcus. Over a length of 100 *km* and of a width of 10 *km*, it reaches elevations of up to 1750 *m*, which is the highest ridge observed on Enceladus so far. Flanking slopes reach 40°. The morphology of the ridge suggests that it formed first by rift flank-uplift caused by extension, but sinistral shear and compression later modified the shape. This modification has in particular emplaced small-scale fragments sticking out of the surface and creating a (previously enigmatic) pattern of black spots on the sun facing side of the ridge. Modelling of uplift related lithospheric flexure yields an effective elastic thickness (T_e) of 0.36 *km* (E=1GPa) at the time of formation, similar to results obtained in Harran Sulcus [1]. Considering the ridge as a load on the lithosphere at present-day, we obtain a lower limit on T_e of 1.5 *km*. Within an asteroid/comet based impact chronology the ridge is 3.6/0.7 Gy old.

1. Introduction

During Cassini's 228th orbit around Saturn the onboard camera imaged, once again, a prominent ridge in Enceladus' Samarkand Sulcus (Fig. 1). This happened because images taken during orbit 3 showed an enigmatic pattern of dark spots on the sun-facing side of the ridge. The new set of images is of higher resolution and, in addition, includes stereo coverage of the surface that provides new 3D information. With that we were able to study the morphology of the ridge in great detail, in particular to ascertain the nature of the dark spots. Moreover, the new observations shed more light on the complex geologic history of Enceladus. Previous papers [2], [3] have concluded that a combination of contraction, extension, and shearing has shaped the ridge, but without being specific. The new data allow narrowing down the formational scenario. Using a stereo-derived topographic model we could also infer information on the state of the lithosphere.

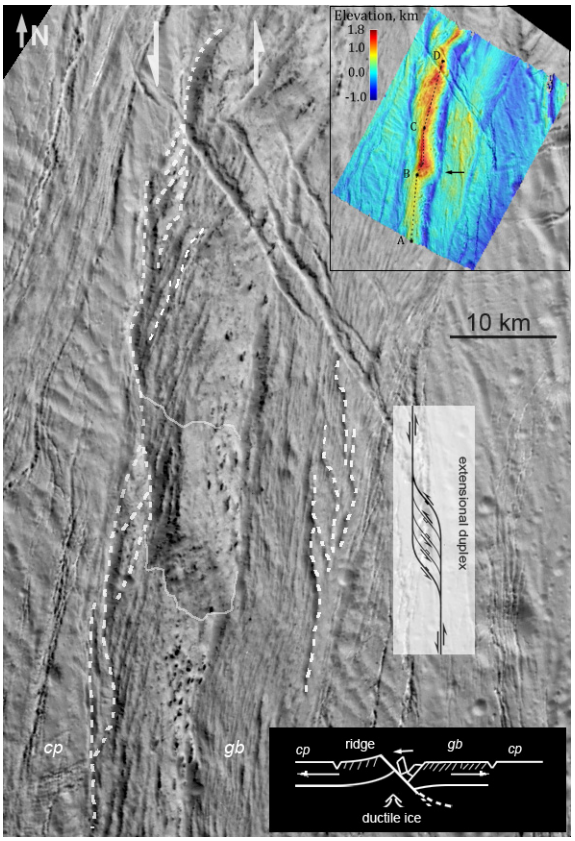

Figure 1: Cut out of Cassini frame N1829240977 (90 *m/pxl*) showing the ridge (centred at 0°, 23°E) and a sketch map of faults (dashed lines) and structural boundaries (thin full lines) identified on the basis of an anaglyph image (not given here). Solar azimuth is 30°. (Top inset) Color-coded Digital Elevation Model (*DEM*) derived from N1829240977 and N1829241569 (60 *m/pxl*) using methods of photogrammetry [1]. *DEM* horizontal resolution is 0.5-1 *km*, vertical accuracy is 30 *m*. (Bottom inset) Cartoon showing how the ridge initially formed. *cp* denotes "cratered plains", and *gb* denotes "grooved band".

2. Observations

(1) The ridge consists of a lower end (Fig. 1, *A*→*B*) and an upper end (*B*→*D*), which stands 600-700 *m* higher on average. There is a distinct boundary between them (Fig. 1, southern full line; Fig. 2, p1).

In addition, the upper end features a second structural boundary (Fig. 1, northern full line) which marks a change in elevation and slope across the ridge (Fig. 2, p5→p6). The highest point of the ridge is 1750 *m* above the surroundings. **(2)** On its eastern side, the ridge is bounded by a pronounced V-shaped trough (Fig. 1, *DEM*). The trough runs roughly straight from south to north and is equally pronounced all the way up. A clear exception is the transition zone between the two ends, where the trough has a narrowing (Fig. 1, black arrow). On its western side, the ridge is bounded by faults with sigmoidal to en echelon patterns (Fig. 1, dashed lines). Compared with the eastern trough, these faults are topographically less pronounced. **(3)** The cross section of the ridge is mostly saw tooth-shaped (Fig. 2, p5-p8) with p5 showing clear indication of flexure of the lithosphere. However, taking p5 as a starting point, there is a growing degree of deformation of the western flank associated with uplifting (p5→p7) and the formation of ramp-like features (p5→p2). Ramps appear to form in relation to the sigmoidal faults (note: p5 lacks a ramp as the bounding fault is shallow there). Ramps can also be observed at the lower end of the ridge (p9, p10). **(4)** While the west facing slope of the ridge is textured as the grooved band to the east (Fig. 1), the east facing slope is not but exhibits a pattern of dark spots. An anaglyph image reveals that most spots are not albedo features but associated with small-scale fragments sticking out of the surface and casting shadows. Consistent with that: image-brightness profiles across different spots show the same constant brightness value in the core of the shadow. **(5)** The grooved band east of the ridge exhibits a fault pattern which is consistent with an extensional duplex at sinistral shear motion (Fig. 1).

3. Discussion and Conclusions

With an elevation of 1750 *m* this ridge is higher than any other ridge observed on Enceladus so far. The ridge summit observed in Harran Sulcus is 1200 *m* (Fig. 2), and the prominent branching dorsa ridges on the trailing hemisphere of Enceladus [3] reach only 900 *m* (result from photoclinometry).

Our observations are consistent with the following formational scenario: The region occupied by the ridge today was initially part of the grooved band (see Fig. 1), which formed by extension. In a late stage of band formation (or soon thereafter), strain focused in the center of the band and created a deep fault and finally a trough. In contrast to the fine-scale faults of the grooved band, this fault has penetrated the lithosphere and thus allowed ductile ice at depth to rise isostatically to the surface. This has flexed the lithosphere and created the saw-tooth shape of the ridge. Subsequently, left lateral shear motion in concert with compression has modified the shape of the ridge, which includes the formation of exceptionally high terrain portions, narrowings, and small-scale fragments sticking out of the surface (dark spots).

Crater size frequency counts yield an age of 3.6/0.7 Gy (asteroid/comet based impact chronology).

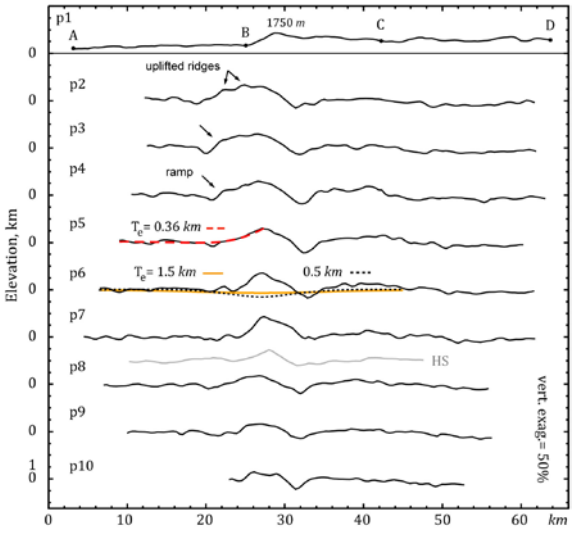

Figure 2: Profiles derived from the *DEM*. p1: along-ridge profile (comp. Fig. 1, top inset). p2-p10: across-ridge, about evenly spaced, profiles with p5 running through point *C* of p1, and p7 including the point of highest elevation. At that point the slope reaches 40°. The grey line is a mean profile across a morphologically similar ridge observed in Harran Sulcus [1]. p5, red dashed line: flexural model profile derived from a bottom loading model [1]. T_e denotes the effective elastic thickness of the lithosphere. p6, orange and dotted line: flexural model profiles derived from a top loading model. Downward flexure with amplitudes >200 *m* would clearly be visible in the data but is not observed (inspect p5, p6, p7). At the given load applied by the ridge this requires $T_e \geq 1.5$ *km*.

References

[1] Giese, B. et al.: Enceladus: An estimate of heat flux and lithospheric thickness from flexurally supported topography, GRL, Vol. 35, L24204, 2008.

[2] Spencer, F. et al.: Enceladus: An Active Cryovolcanic Satellite, in *Saturn from Cassini-Huygens*, Springer Netherlands, 683-724, 2009.

[3] Crow-Willard, E. N., and R. T. Pappalardo: Structural mapping of Enceladus and implications for formation of tectonized regions, JGR, Planets, 120, 928–950, 2015.